Int. J. Therm. Sci. (2000) 39, 635–644

S1290-0729(00)00227-1/FLA

Flow of viscous incompressible fluid with temperature dependent viscosity and thermal conductivity past a permeable wedge with uniform surface heat flux

Md. Anwar Hossain [a]*, Md. Sazzad Munir [a], David Andrew S. Rees [b]

[a] *Department of Mathematics, University of Dhaka, Dhaka 1000, Bangladesh*

[b] *Department of Mechanical Engineering, University of Bath, Bath BA2 7AY, England, UK*

(Received 23 August 1999, accepted 30 November 1999)

Abstract — We consider a steady two-dimensional laminar forced flow and heat transfer of a viscous incompressible fluid having temperature dependent viscosity and thermal conductivity past a wedge with a uniform surface heat flux. The governing equations, reduced to local nonsimilarity boundary layer equations using suitable transformations, have been integrated employing an implicit finite difference method. Perturbation techniques are employed to obtain the solutions near the leading edge as well as far from it. The perturbation solutions are compared with the finite difference solutions and found to be in excellent agreement. The results are presented in terms of local skin friction coefficient and rate of heat transfer for various values of the governing parameters, such as the Prandtl number Pr, the pressure gradient parameter m, the viscosity variation parameter ε and thermal conductivity variation parameter γ, against the local permeability parameter ξ. The effect of variations in ξ, ε and γ on the dimensionless velocity, viscosity and thermal conductivity distributions are also depicted graphically for $Pr = 0.7$. © 2000 Éditions scientifiques et médicales Elsevier SAS

heat transfer / laminar forced flow / wedge flow / uniform heat flux / temperature dependent viscosity and thermal conductivity

Nomenclature

x	streamwise coordinate	m
y	transverse coordinate	m
u	velocity component in the x-direction	$\mathrm{m\cdot s^{-1}}$
v	velocity component in the y-direction	$\mathrm{m\cdot s^{-1}}$
f	dimensionless stream function	
β	angle factor of the wedge	
T	temperature of the fluid	K
T_∞	temperature of the ambient fluid	K
T_w	wall temperature	K
Pr	Prandtl number	
Re_x	local Reynolds number	
Nu_x	Nusselt number	
C_f	the skin friction	
Ω	total angle of the wedge	
c_p	specific heat	$\mathrm{J\cdot kg^{-1}\cdot k^{-1}}$
ψ	stream function	$\mathrm{m^2\cdot s^{-1}}$
θ	dimensionless temperature function	
ξ	suction parameter	
η	similarity variable	
m	pressure gradient parameter	
q_w	wall heat flux	$\mathrm{W\cdot m^{-2}}$
U_∞	potential flow velocity	$\mathrm{m\cdot s^{-1}}$
V_w	suction velocity	
ρ	fluid density	$\mathrm{kg\cdot m^{-3}}$
ν	the kinematic coefficient of viscosity	$\mathrm{m^2\cdot s^{-1}}$
μ	dynamic viscosity of the fluid	$\mathrm{kg\cdot m^{-1}\cdot s^{-1}}$
μ_∞	dynamic viscosity of the ambient fluid	$\mathrm{kg\cdot m^{-1}\cdot s^{-1}}$
ε	viscosity variation parameter	
κ	thermal conductivity	$\mathrm{W\cdot m^{-1}\cdot K^{-1}}$
κ_∞	thermal conductivity of the ambient fluid	$\mathrm{W\cdot m^{-1}\cdot K^{-1}}$
γ	thermal conductivity variation	

* Correspondence and reprints.
anwar@du.bangla.nd

1. INTRODUCTION

Steady two-dimensional laminar forced flow and heat transfer from a wedge was considered in great detail by Lin et al. [1]. They proposed a similarity solution for an isothermal surface as well as for a uniform heat flux surface for a wide range of Prandtl numbers. If the effect of surface suction/blowing is included, a similarity solution is possible only when the suction/blowing rate is proportional to $x^{(m-1)/2}$ [2], where x is the distance from the leading edge and m is the pressure gradient parameter. Koh and Hartnett [3] studied the incompressible laminar flow over a porous wedge with suction and a variable wall temperature. They obtained similarity solutions for wall temperature and the suction rate variations which are proportional to a power of x. From the practical point of view, a uniform transpiration velocity may be more easily realized than an $x^{(m-1)/2}$ distribution. Watanabe [4] investigated thermal boundary layer flow over a uniform surface temperature wedge with a transpiration velocity in forced flow. Yih [5] extended the above problem by considering the heat transfer characteristics in the forced flow over a wedge subjected to a uniform wall heat flux.

All the above investigations were carried out for the fluids having uniform viscosity throughout the flow regime. However, it is known that this physical property may change significantly with temperature. Gary et al. [6] and Mehta and Sood [7] found that the flow characteristics substantially change due to the consideration of temperature dependent viscosity. Mindful of this, Hady et al. [8], Kafoussias and Williams [9] and Kafoussias and Rees [10] have investigated the effect of temperature dependent viscosity on the mixed convection flow from a vertical flat plate in the region near the leading edge. Very recently Severin and Herwig [11, 12] investigated the Rayleigh–Benard convection flow with fluid having temperature dependent viscosity using the appropriate asymptotic analysis. For a fluid with viscosity inversely proportional to the temperature the problems of mixed convection flow from a vertical heated flat plate, of natural convection flow from a vertical wavy surface and a vertical truncated cone and a wedge has, recently, been investigated by Hossain et al. [13–16].

For liquid metals, it has been found that the thermal conductivity κ varies with temperature in an approximately linear manner in the range from 0 °F to 400 °F (see Kays [17]) and a semi-empirical formula for the thermal conductivity of the aforementioned form was deduced by Arunachalam et al. [18]. Considering the thermal conductivity of the fluid proportional to a linear function of temperature Chiam [19] investigated the effect of a variable thermal conductivity on the flow and heat transfer from a linearly stretching sheet.

In the present study we investigate the effect of uniform transpiration velocity on the flow and heat transfer of a viscous incompressible fluid having temperature dependent viscosity as well as thermal conductivity past a wedge. The surface of the wedge is maintained with uniform surface heat flux. The various configurations of wedge from Blasius flow ($m = 0$) to Hiemenz flow ($m = 1$) have been considered in this investigation. In formulating the equations governing the flow both the viscosity and the thermal conductivity of the fluid are considered to be a linear function of temperature (see Charradeau [20]). The governing partial differential equations are reduced to locally nonsimilar partial differential equations by introducing the transformations appropriate for the forced flow past a wedge. Solutions of these equations are obtained by three distinct methodologies; namely, the perturbation method for small values of the transpiration parameter ξ, the asymptotic solutions for large values ξ and an implicit finite difference method for all values of ξ. Variations of the local skin-friction and the local Nusselt number and their dependence on changes in the viscosity-variation parameter ε, thermal conductivity variation parameter γ, and the pressure gradient parameter m are shown in tabular form against ξ for different values of Pr. The effects of variations in both ε and ξ on the velocity and the viscosity distribution are shown graphically, for a fluid having the value of $Pr = 0.7$ that is appropriate for helium (400 °F), hydrogen (near about 370 °F) and oxygen (near about 10 °F).

2. MATHEMATICAL FORMALISM

We consider the steady two-dimensional laminar flow of a viscous incompressible fluid with temperature dependent viscosity and thermal conductivity past a wedge. A schematic diagram illustrating the flow domain and the coordinate system is given in *figure 1*. According to the assumption, the two-dimensional boundary layer equations for the flow of the fluid past a wedge are as follows (*system of a wedge*):

$$\frac{\partial u}{\partial x} + \frac{\partial v}{\partial y} = 0 \tag{1}$$

$$u\frac{\partial u}{\partial x} + v\frac{\partial u}{\partial y} = U_\infty \frac{\mathrm{d}U_\infty}{\mathrm{d}x} + \frac{1}{\rho}\frac{\partial}{\partial y}\left(\mu\frac{\partial u}{\partial y}\right) \tag{2}$$

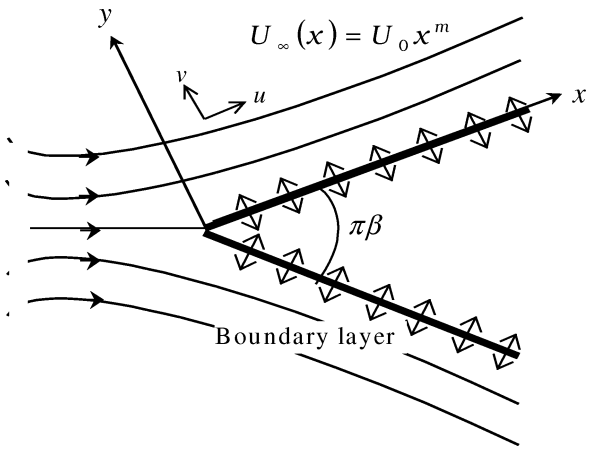

Figure 1. The flow configuration and the coordinate.

$$u\frac{\partial T}{\partial x} + v\frac{\partial T}{\partial y} = \frac{1}{\rho c_p}\frac{\partial}{\partial y}\left(\kappa\frac{\partial T}{\partial y}\right) \tag{3}$$

where u, v are fluid velocity components in the x- and y-direction, respectively, T is the temperature of the fluid in the boundary layer region; $U_\infty(x)$ being the free stream velocity. μ and κ are respectively the dynamic viscosity and the thermal conductivity, following [20], which are given as below:

$$\mu = \mu_\infty\left[1 + \alpha_1\frac{T - T_\infty}{T_0 - T_\infty}\right] \tag{4a}$$

and

$$\kappa = \kappa_\infty\left[1 + \alpha_2\frac{T - T_\infty}{T_0 - T_\infty}\right] \tag{4b}$$

In (4) μ_∞ is the viscosity and κ_∞ is the thermal conductivity of the ambient fluid, T_∞ is the temperature of the ambient fluid, T_0 is some reference temperature and α_1 and α_2 are constants. Clearly $\alpha_1 = 0$ and $\alpha_2 = 0$ represent that the dynamical viscosity and the thermal conductivity be uniform.

Solutions of the above equations have to satisfy the following boundary conditions:

$$\begin{aligned} &u = 0, \qquad v = -V_\mathrm{w}, \qquad -\kappa_\infty\left(\frac{\partial T}{\partial y}\right)_{y=0} = q_\mathrm{w} \\ &\quad \text{at } y = 0 \\ &u \to U_\infty = U_0 x^m, \qquad T \to T_\infty \\ &\quad \text{as } y \to \infty \end{aligned} \tag{5}$$

where V_w is the transpiration velocity, which is positive for suction or withdrawal and negative for injection or blowing of fluid through the wedge surface; U_0 is the constant velocity of the potential flow outside the boundary layer, $m = \beta/(2-\beta)$, and β is the Hartee pressure gradient parameter which is related to the total angle of the wedge, Ω, by $\Omega = \pi\beta$.

Now we define the following dimensionless variables:

$$\begin{aligned} \psi &= \nu_\infty\sqrt{\frac{2}{1+m}}Re_x^{1/2}\left[f(\xi,\eta) + \frac{1+m}{2}\xi\right] \\ T - T_\infty &= \sqrt{\frac{2}{m+1}}\,\frac{q_\mathrm{w}x}{k_\infty}Re_x^{-1/2}\theta(\xi,\eta) \\ \eta &= \sqrt{\frac{m+1}{2}}\,\frac{y}{x}Re_x^{1/2} \\ \xi &= \sqrt{\frac{2}{m+1}}\,\frac{V_\mathrm{w}x}{\nu_\infty}Re_x^{-1/2} \end{aligned} \tag{6}$$

where ψ is the stream function that satisfies the continuity equation, $f(\xi,\eta)$ is the dimensionless stream function, η is pseudo-similarity variable, $\theta(\xi,\eta)$ is the dimensionless temperature of the fluid in the boundary layer region, where $\nu_\infty = \mu_\infty/\rho$ is the free stream kinematic viscosity, $Re_x = U_\infty x/\nu_\infty$ is the local Reynolds number and ξ is termed as the local transpiration parameter which is positive and negative according as when fluid being sucked and injected through the surface.

Substituting the transformation given in (6) into (2)–(3) one obtains the following nonsimilar system of equations governing the flow and the energy transport:

$$\begin{aligned} &(1+\varepsilon\xi\theta)f''' + \varepsilon\xi\theta' f'' + ff'' + \frac{2m}{1+m}\left(1 - f'^2\right) + \xi f'' \\ &\quad = \frac{1-m}{1+m}\xi\left(f'\frac{\partial f'}{\partial\xi} - f''\frac{\partial f}{\partial\xi}\right) \end{aligned} \tag{7}$$

$$\begin{aligned} &\frac{1}{Pr}(1+\gamma\xi\theta)\theta'' + \gamma\xi\theta'^2 + f\theta' - \frac{1-m}{1+m}\theta f' + \xi\theta' \\ &\quad = \frac{1-m}{1+m}\xi\left(f'\frac{\partial\theta}{\partial\xi} - \theta'\frac{\partial f}{\partial\xi}\right) \end{aligned} \tag{8}$$

In equations (7) and (8), $\varepsilon = \alpha_1 Nu_x/Re_\mathrm{s}$ and $\gamma = \alpha_2 Nu_x/Re_\mathrm{s}$ are termed as the viscosity-variation parameter and the thermal conductivity-variation parameter; where Nu_x is the Nusselt number defined in equation (10) and $Re_\mathrm{s} = V_\mathrm{w}x/\nu_\infty$ is the Reynolds number due to blowing/injection of fluid through the surface.

The boundary conditions appropriate for the above equations are

$$\begin{aligned} &f(\xi,0) = f'(\xi,0) = 0, \qquad &&\theta'(\xi,0) = -1 \\ &f'(\xi,\infty) = 1, &&\theta(\xi,\infty) = 0 \end{aligned} \tag{9}$$

It can be seen that throughout consideration of $\varepsilon = \gamma = 0$, the problem reduces to that investigated by Yih [5]. Using the local nonsimilarity method the author obtained the solution valid in the region near the leading edge.

Here we are proposing to simulate the system of equations (7) and (8) subject to the boundary conditions (9) by means of the implicit finite difference method, which has been used, recently, by Hossain et al. [13–16]. In introducing this method, the system of partial differential equations (7) and (8) are first converted to a system of first order partial differential equations by introducing new functions of η and η-derivatives. This system is then approximated using finite-difference scheme and the resulting nonlinear system of difference equations is linearized by the use of Newton's quasi-linearization method. These linear difference equations, along with the boundary conditions (9), are finally solved by an efficient block-tridiagonal factorization method based on the well-known Thomas algorithm. The whole procedure was first introduced by Keller [21] and is known as Keller's box method.

Once we know the values of the functions $f(\xi,\eta)$ and $\theta(\xi,\eta)$ and their derivatives, it becomes important to calculate the values of the local skin-friction C_{fx} and the local Nusselt number Nu_x which are defined by

$$C_{fx} = \frac{\tau_w x}{(1/2)\rho U_\infty^2} \quad \text{and} \quad Nu_x = \frac{q_w x}{\kappa_\infty (T_0 - T_\infty)} \tag{10}$$

where τ_w is the shearing stress at the surface defined by

$$\tau_w = \mu_\infty \left(\frac{\partial u}{\partial y}\right)_{y=0} \tag{11}$$

Now incorporating the transformations given in (6) in the foregoing relations, the following relations for the skin-friction and the Nusselt number hold:

$$\frac{1}{\sqrt{2}(1+m)} C_{fx} Re_x^{1/2} = f''(\xi,0) \tag{12a}$$

and

$$\sqrt{\frac{2}{1+m}}\,\frac{Nu_x}{Re_x^{1/2}} = \frac{1}{\theta(\xi,0)} \tag{12b}$$

Results obtained by the Keller box method are presented in *tables I–IV*. In *tables II* and *III* the results are compared with the solutions obtained by other methods discussed below.

TABLE I
Values of $Nu_x/Re_x^{1/2}$ for different $Pr = 0.1, 1.0, 10.0$ at $\varepsilon = 0.0$, $\gamma = 0.0$ and $\xi = 0.0$ while $m = 0.0, 1/3, 1.0$.

M	0.0		1/3		1.0	
Pr	Yih [5]	Present	Yih [5]	Present	Yih [5]	Present
10.0	0.9978	0.9978	1.23177	1.2317	1.33879	1.3387
1.0	0.4589	0.4589	0.54197	0.5419	0.57046	0.5704
0.1	0.2006	0.2006	0.21947	0.2193	0.21950	0.2195

2.1. Solution for small ξ

Since ξ is small near the leading edge, solutions of the equations (7)–(9) may be obtained by using the perturbation method. Hence, we expand the functions $f(\xi,\eta)$ and $\theta(\xi,\eta)$ in powers of ξ as given below:

$$f(\xi,\eta) = \sum_{i=0}^{\infty} \xi^i f_i(\eta) \quad \text{and} \quad \theta(\xi,\eta) = \sum_{i=0}^{\infty} \xi^i \theta_i(\eta) \tag{13}$$

Now, on substituting the above expansions in equations (7)–(9) and taking the terms up to $O(\xi^2)$ we get

$$f_0''' + f_0 f_0'' + \frac{2m}{1+m}\left(1 - f_0'^2\right) = 0 \tag{14}$$

$$\frac{1}{Pr}\theta_0'' + f_0\theta_0' - \frac{1-m}{1+m}\theta_0 f_0' = 0 \tag{15}$$

$$\begin{aligned} &f_0(0) = f_0'(0) = 0, \qquad \theta_0'(0) = -1 \\ &f_0'(\infty) = 1, \qquad\qquad \theta_0(\infty) = 0 \end{aligned} \tag{16}$$

$$f_1''' + \varepsilon\left(\theta_0 f_0''' + \theta_0' f_0''\right) + f_0 f_1'' + \frac{1}{1+m} f_1 f_0'' + f_0'' - \frac{1+3m}{1+m} f_1' f_0' = 0 \tag{17}$$

$$\frac{1}{Pr}\theta_1'' + \frac{1}{Pr}\gamma\left(\theta_0\theta_0'' + \theta_0'^2\right) + f_0\theta_1' + \frac{2}{1+m} f_1\theta_0' - \frac{1-m}{1+m}\theta_0 f_1' - \frac{2(1-m)}{1+m}\theta_1 f_0' + \theta_0' = 0 \tag{18}$$

$$\begin{aligned} &f_1(0) = f_1'(0) = \theta_1'(0) = 0 \\ &f_1'(\infty) = \theta_1(\infty) = 0 \end{aligned} \tag{19}$$

$$f_2''' + \varepsilon\left(\theta_0 f_1''' + \theta_1 f_0''' + \theta_0' f_1'' + \theta_1' f_0''\right) + f_0 f_2'' + \frac{2}{1+m} f_1\theta_1' + \frac{3-m}{1+m} f_2\theta_0' + \theta_1' - \frac{1-m}{1+m}\theta_0 f_2' = 0 \tag{20}$$

TABLE II
Values of the local skin friction coefficient $C_{fx}Re_x^{1/2}/(\sqrt{2}(1+m))$ for different ξ at $\varepsilon = 0.0, 0.5$ and $\gamma = 0.0, 0.5$ while $m = 0.5$ and $Pr = 0.7$.

ξ	$\varepsilon = 0.0$				$\varepsilon = 0.5$			
	$\gamma = 0.0$		$\gamma = 0.5$		$\gamma = 0.0$		$\gamma = 0.5$	
	Small & large ξ	Finite diff.	Small & large ξ	Finite diff.	Small & large ξ	Finite diff.	Small & large ξ	Finite diff.
0.0	1.0389[s]	1.0388	1.0389[s]	1.0388	1.0389[s]	1.0388	1.0389[s]	1.0388
0.2	1.1540[s]	1.1581	1.1540[s]	1.1581	1.0378[s]	1.0488	1.0378[s]	1.0409
0.4	1.2692[s]	1.2849	1.2692[s]	1.2849	1.0368[s]	1.0762	1.0368[s]	1.0478
0.6	1.3843[s]	1.4189	1.3843[s]	1.4189	1.0358[s]	1.1166	1.0358[s]	1.0586
0.8	1.4995[s]	1.5593	1.4995[s]	1.5593	1.0348[s]	1.1674	1.0348[s]	1.0725
1.0	1.6146[s]	1.7055	1.6146[s]	1.7055	1.0338[s]	1.2266	1.0338[s]	1.0891
2.0	2.6666[a]	2.5059	2.6666[a]	2.5059	1.7263[a]	1.6100	1.3820[a]	1.2026
4.0	4.3333[a]	4.3047	4.3333[a]	4.3047	2.6135[a]	2.5925	1.5482[a]	1.5426
6.0	6.2222[a]	6.2129	6.2222[a]	6.2129	3.6871[a]	3.6784	1.9846[a]	1.9865
8.0	8.1666[a]	8.1624	8.1666[a]	8.1624	4.8074[a]	4.8003	2.4885[a]	2.4875
10.0	10.1333[a]	10.131	10.1333[a]	10.131	5.9463[a]	5.9377	3.0195[a]	3.0157

[s] for small ξ.
[a] for large ξ.

$$\frac{1}{Pr}\theta_2'' + \gamma\left(\theta_0\theta_1'' + \theta_1\theta_0'' + 2\theta_1'\theta_0'\right) + f_0\theta_2' - \frac{2(1-m)}{1+m}\theta_1 f_1' - \frac{3(1-m)}{1+m}\theta_2 f_0' = 0 \quad (21)$$

$$\begin{aligned} f_2(0) = f_2'(0) = \theta_2'(0) = 0 \\ f_2'(\infty) = \theta_2(\infty) = 0 \end{aligned} \quad (22)$$

It can be seen that equations (12) are the very well known Falkner–Skan boundary layer equations, solutions of which are available in the literature for different values of m that measure the wedge angle. Hence later equations are linear and can be solved easily. Here solutions of the subsequent equations are obtained by using the Nachtscheim–Swigert iteration technique together with the sixth order implicit Runge–Kutta–Butcher initial value solver.

When we know the value of $f_i(\eta)$ and $\theta_i(\eta)$ for $i = 0, 1, 2, \ldots$ and their derivatives, we can calculate the values of local skin-friction and the local Nusselt number from the expressions given below:

$$\frac{1}{\sqrt{2}(1+m)} C_{fx}Re_x^{1/2} = f_0''(0) + \xi f_1''(0) + O\left(\xi^2\right) \quad (23)$$

and

$$\sqrt{\frac{2}{1+m}}\,\frac{Nu_x}{Re_x^{1/2}} = \frac{1}{\theta_0(0) + \xi\theta_1(0) + O(\xi^2)} \quad (24)$$

For example, for $Pr = 0.7$, $m = 0.5$, $\varepsilon = 0.5$ and $\gamma = 0.5$ the numerical values of the local skin-friction and the local rate of heat transfer for different values of ξ can be obtained from the following expressions:

$$\frac{C_{fx}Re_x^{1/2}}{\sqrt{2}(1+m)} = 1.03890 - 0.00503\xi + \cdots \quad (25)$$

and

$$\frac{\sqrt{2}\,Nu_x}{\sqrt{(1+m)}Re_x} = \frac{1}{1.78420 - 0.23565\xi + \cdots} \quad (26)$$

The resulting values of the local skin-friction coefficient and the local Nusselt number are entered in *tables II* and *III*, and compared with the corresponding values obtained from finite difference solution.

2.2. Solution for large ξ

Here attention shall be given to the behavior of the solutions to the equations (7) and (8) when ξ is large. An order of magnitude analysis of the various terms in these equations shows that the largest are $\xi f''$ in (7) and $\xi\theta'$ in (8). In their respective equations, both terms have to be balanced and the only way to do this is to assume that η is small, and hence that η derivatives are large. Given that $\theta = O(\xi^{-1})$ as $\xi \to \infty$, it is necessary to

TABLE III
Values of the local Nusselt number, $\sqrt{2}Nu_x/((1+m)Re_x)^{1/2}$, for different ξ at $\varepsilon = 0.0, 0.5$ and $\gamma = 0.0, 0.5$ while $m = 0.5$ and $Pr = 0.7$.

ξ	$\varepsilon = 0.0$				$\varepsilon = 0.5$			
	$\gamma = 0.0$		$\gamma = 0.5$		$\gamma = 0.0$		$\gamma = 0.5$	
	Small & large ξ	Finite diff.	Small & large ξ	Finite diff.	Small & large ξ	Finite diff.	Small & large ξ	Finite diff.
0.0	0.5604[s]	0.5605	0.5604[s]	0.5605	0.5604[s]	0.5605	0.5604[s]	0.5605
0.2	0.6503[s]	0.6412	0.5875[s]	0.5861	0.6357[s]	0.6314	0.5756[s]	0.5756
0.4	0.7744[s]	0.7280	0.6174[s]	0.6115	0.7344[s]	0.7108	0.5917[s]	0.5914
0.6	0.9570[s]	0.8208	0.6504[s]	0.6368	0.8692[s]	0.7981	0.6087[s]	0.6080
0.8	1.2524[s]	0.9190	0.6872[s]	0.6620	1.0648[s]	0.8926	0.6266[s]	0.6253
1.0	1.8116[s]	1.0223	0.7284[s]	0.6872	1.3739[s]	0.9936	0.6457[s]	0.6433
2.0		1.5974		0.8147		1.5699		0.7453
4.0	2.9072[a]	2.8984	1.2293[a]	1.0896	2.8838[a]	2.8823	1.0397[a]	1.0077
6.0	4.2764[a]	4.2612	1.4205[a]	1.4022	4.2559[a]	4.2505	1.3371[a]	1.3336
8.0	5.6636[a]	5.6402	1.7532[a]	1.7476	5.6426[a]	5.6323	1.6980[a]	1.6950
10.0	7.0576[a]	7.0248	2.1186[a]	2.1135	7.0350[a]	7.0185	2.0768[a]	2.0722

[s] for small ξ.
[a] for large ξ.

find the appropriate scaling for f and η. On balancing the f''' and $\xi f''$ terms in (7), it is found that $\eta = \mathrm{O}(\xi)$ and $f = \mathrm{O}(\xi^{-1})$ as $\xi \to \infty$. Therefore, the following substitutions are made to the dependent and independent variables:

$$f = \xi^{-1}\hat{f} = 0, \qquad \theta = \xi^{-1}\hat{\theta}, \qquad \hat{\eta} = \xi\eta \tag{27}$$

Substituting this transformation into equations (7)–(9) and dropping the hats for brevity, these yield the following equations:

$$(1+\varepsilon\theta)f''' + \varepsilon\theta' f'' + \frac{2m}{1+m}\xi^{-2}\left[ff'' + 1 - f'^2\right] + (1+\varepsilon\theta)^2 f'' = \frac{1-m}{1+m}\xi^{-1}\left(f'\frac{\partial f'}{\partial\xi} - f''\frac{\partial f}{\partial\xi}\right) \tag{28}$$

$$\frac{1}{Pr}(1+\gamma\theta)\theta'' + \frac{1}{Pr}\gamma\theta'^2 + \theta' + \frac{2m}{1+m}\xi^{-2}f\theta' = \frac{1-m}{1+m}\xi^{-1}\left(f'\frac{\partial\theta}{\partial\xi} - \theta'\frac{\partial f}{\partial\xi}\right) \tag{29}$$

The corresponding boundary conditions are

$$\begin{aligned} &f(\xi,0) = f'(\xi,0) = 0, && \theta'(\xi,0) = -1 \\ &f'(\xi,\infty) = 1, && \theta(\xi,\infty) = 0 \end{aligned} \tag{30}$$

Since ξ is large, solutions of the equations (22)–(23) may be obtained by using a straightforward perturbation method. Hence, we expand the functions $f(\xi,\eta)$ and $\theta(\xi,\eta)$ in powers of ξ as given below:

$$\begin{aligned} f(\xi,\eta) &= \sum_{i=0}^{\infty}\xi^{-2i}f_i(\eta) \\ \theta(\xi,\eta) &= \sum_{i=0}^{\infty}\xi^{-2i}\theta_i(\eta) \end{aligned} \tag{31}$$

Now, on substituting the above expansions into equations (7) and (9) and taking terms up to $\mathrm{O}(\xi^{-1})$ we get

$$(1+\varepsilon\theta_0)f_0''' + \varepsilon\theta_0' f_0'' + f_0'' = 0 \tag{32}$$

$$\frac{1}{Pr}(1+\gamma\theta_0)\theta_0'' + \frac{1}{Pr}\gamma\theta_0'^2 + \theta_0' = 0 \tag{33}$$

$$\begin{aligned} &f_0(0) = f_0'(0) = 0, && \theta_0'(0) = -1 \\ &f_0'(\infty) = 1, && \theta_0(\infty) = 0 \end{aligned} \tag{34}$$

$$(1+\varepsilon\theta_0)f_1''' + \varepsilon\left(\theta_1' f_0''' + f_1''\theta_0' + f_0''\theta_1'\right) + \left(\frac{2m}{1+m}f_0 f_0'' + \frac{2m}{1+m}\left(1 - f_0'^2\right) + f_1''\right) = 0 \tag{35}$$

$$\frac{1}{Pr}(1+\gamma\theta_0)\theta_1'' + \frac{1}{Pr}\gamma\left(\theta_1\theta_0'' + 2\theta_1'\theta_0'\right) + \theta_1' + \frac{2m}{1+m}f_0\theta_0' = 0 \tag{36}$$

TABLE IV
The values of $C_{fx}Re_x^{1/2}/(\sqrt{2}(1+m))$ and $\sqrt{2}\,Nu_x/((1+m)Re_x)^{1/2}$ for different ξ at $m=0.5$, $\varepsilon=0.5$ and $\gamma=0.5$ while $Pr=0.1, 1.0, 7.0, 10.0$.

	$C_{fx}Re_x^{1/2}/(\sqrt{2}(1+m))$				$\sqrt{2}\,Nu_x/((1+m)Re_x)^{1/2}$			
ξ	$Pr=0.1$	$Pr=1.0$	$Pr=7.0$	$Pr=10.0$	$Pr=0.1$	$Pr=1.0$	$Pr=7.0$	$Pr=10.0$
0.0	1.04784	1.03887	1.03886	1.03886	0.32638	0.64199	1.30022	1.47378
0.5	0.86995	1.09556	1.27195	1.29198	0.24728	0.76233	3.56618	4.99378
1.0	0.73126	1.19487	1.59173	1.62400	0.20811	0.90255	6.61359	9.58269
2.0	0.58697	1.48143	2.33040	2.38196	0.17883	1.24597	13.04423	19.02956
4.0	0.48302	2.27068	3.99743	4.08852	0.16337	2.10948	26.00454	37.97893
6.0	0.44229	3.17838	5.76625	5.89843	0.15819	3.05657	38.95710	56.88769
8.0	0.41941	4.12405	7.57237	7.74624	0.15519	4.02089	51.87644	75.71991
10.0	0.40136	5.08458	9.39434	9.61009	0.15362	4.98837	64.74823	94.44832

$$f_1(0)=f_1'(0)=\theta_1'(0)=0$$
$$f_1'(\infty)=\theta_1(\infty)=0 \tag{37}$$

$$(1+\varepsilon\theta_0)f_2'''+\varepsilon\left(\theta_1 f_1'''+\theta_2 f_0'''+\theta_2' f_0''+\theta_1' f_1''+\theta_0 f_2''\right)+f_2''+\frac{2m}{1+m}f_0 f_1''+\frac{2(2m-1)}{1+m}f_1 f_0''+\frac{2(3m-1)}{1+m}f_1' f_0'=0 \tag{38}$$

$$\frac{1}{Pr}(1+\gamma\theta_0)\theta_2''+\frac{1}{Pr}\gamma\left(\theta_1\theta_1''+\theta_2\theta_0''+\theta_1'^2+2\theta_2'\theta_0'\right)+\theta_2'+\frac{2m}{1+m}f_0\theta_1'-\frac{2(1-m)}{1+m}f_0'\theta_1+f_1\theta_0'=0 \tag{39}$$

$$f_2(0)=f_2'(0)=\theta_2'(0)=0$$
$$f_2'(\infty)=\theta_2(\infty)=0 \tag{40}$$

The solution methodology applied in solving the above sets of equations is the same as for the solution of the small ξ equations. As before, when we know the values of the functions $f_i(\xi,\eta)$ and $\theta_i(\xi,\eta)$ (for $i=0$ and 1) and their derivatives, we can calculate the asymptotic values of the local skin-friction and the local Nusselt number from the following relations:

$$\frac{1}{\sqrt{2}(1+m)}C_{fx}Re_x^{1/2}=\xi\left[f_0''(\xi,0)+\xi^{-2}f_1''(\xi,0)+\cdots\right] \tag{41}$$

and

$$\sqrt{\frac{2}{1+m}}\,\frac{Nu_x}{Re_x^{1/2}}=\frac{\xi}{\theta_0(\xi,0)+\xi^{-2}\theta_1(\xi,0)+\cdots} \tag{42}$$

These asymptotic solutions are compared with the solution of the finite difference method in *tables II* and *III*.

Further, for the above three sets of equations (28)–(36) it can be seen that when $\varepsilon=0$ and $\gamma=0$, the analytical solution becomes straightforward; these have been given in Hossain et al. [16].

3. RESULTS AND DISCUSSION

Here we have investigated the problem of the forced convective flow and heat transfer of a viscous incompressible fluid with variable viscosity and thermal conductivity past a wedge with uniform surface mass-flux. Solutions are obtained for fluids having Prandtl number $Pr=0.1, 0.7, 1.0, 7.0, 10.0$ and for a wide range of values of the variable viscosity parameter $\varepsilon=0.0$, 1, 2.5 and 5.0.

Numerical values of $\sqrt{2}\,Nu_x/((1+m)Re_x)^{1/2}$ are depicted in *table I* for $Pr=0.1$, 1.0 and 10.0 at $\varepsilon=0.0$ and for various values of $m=0.0, 1/3, 1.0$. Suitable comparisons with the results of Yih [5] show excellent agreement between these two solutions. Here we have found that the value of $\sqrt{2}\,Nu_x/((1+m)Re_x)^{1/2}$ increases whenever the value of the pressure gradient parameter m increases at a given value of Pr. We also observe that if Pr decreases, then there is a corresponding decrease in the value of local Nusselt number for fixed value of m that means the boundary layer thickness increasing with the increase of Pr.

The numerical values of the local skin-friction $C_{fx}Re_x^{1/2}/(\sqrt{2}(1+m))$ and the local Nusselt number $\sqrt{2}\,Nu_x/((1+m)Re_x)^{1/2}$ for various values of ξ on taking $\varepsilon=0.0, 0.5$ and $\gamma=0.0, 0.5$ while $Pr=0.7$ and $m=0.5$, which were obtained by the finite-difference method, are displayed in *tables II* and *III*. In these tables, we have also entered the solutions obtained from

the perturbation solution for small values of ξ and the asymptotic solutions obtained for large values of ξ. The comparison between the latter solutions to the finite-difference solutions for a very large range of ξ values is found to be excellent. From these tables we may observe that in the entire ξ range the local skin friction coefficient $C_{fx}Re_x^{1/2}/(\sqrt{2}(1+m))$ and the local Nusselt number $\sqrt{2}Nu_x/((1+m)Re_x)^{1/2}$ increase due to increases in ξ and ε, and decreases in γ. But when $\varepsilon = 0.0$ there is no increase or decrease in $C_{fx}Re_x^{1/2}/(\sqrt{2}(1+m))$ with increase of γ, which is expected.

To investigate the flow behavior with increasing values of Pr, we have entered the numerical values of $C_{fx}Re_x^{1/2}/(\sqrt{2}(1+m))$ and $\sqrt{2}Nu_x/((1+m)Re_x)^{1/2}$ in *table IV*, for various ξ on taking $Pr = 0.1, 0.7, 1.0, 7.0$ while $m = 0.5$, $\varepsilon = 0.5$ and $\gamma = 0.5$, as obtained by the finite difference method. In these tables, we have also shown the solution obtained from the perturbation solution for small values of ξ and the asymptotic solutions for large values of ξ. The comparison between the latter solutions and the finite-difference solutions for entire ξ range are again excellent. From this table it may found that, in the entire ξ range, both the local skin-friction $C_{fx}Re_x^{1/2}/(\sqrt{2}(1+m))$ and the local Nusselt number $\sqrt{2}Nu_x/((1+m)Re_x)^{1/2}$ increase due to increases in both ξ and Pr. It should be noticed that for low Prandtl number, for example, for $Pr = 0.1$ both $C_{fx}Re_x^{1/2}/(\sqrt{2}(1+m))$ and $\sqrt{2}Nu_x/((1+m)Re_x)^{1/2}$ decrease with increasing values of ξ.

Now we discuss the effect of the viscosity-variation parameter ε, thermal conductivity parameter γ and the local suction parameter ξ on the velocity, the viscosity and thermal conductivity profiles obtained by the finite difference solutions.

The effect of changes in the viscosity variation parameter, $\varepsilon = 0.0, 1.0, 2.5, 5.0$, on the dimensionless velocity function u/U_∞ and viscosity function μ/μ_∞ against η at $\xi = 1.0, 5.0, 10.0$ for a fluid with $Pr = 0.7$, $m = 0.5$ and $\gamma = 0.5$ is shown in *figures 2(a)* and *2(b)*. In these figures the solid, dashed and dotted curves are used to represent the aforementioned physical variables for $\xi = 10.0$, $\xi = 5.0$ and $\xi = 1.0$, respectively. From *figure 2(a)* it can be seen that the velocity of the fluid decreases with an increase in the viscosity-variation parameter ε. We also observe that the velocity of the fluid increases near the surface of the wedge. On the other hand, from *figure 2(b)* it can be seen that an increase in the viscosity-variation parameter ε also leads to a greater viscosity distribution. For fixed ε this decreases near the surface of the wedge and with the increase of η asymptotic to unit value at the outer edge of the boundary layer for all ξ and that is expected. For the interest of the experimentalist, we show the percentage changes in the velocity and viscosity with the increase of viscosity variation parameter. For example, at $Pr = 0.7$, $m = 0.5$, $\gamma = 0.5$, $\xi = 10.0$ and $\eta = 0.2$

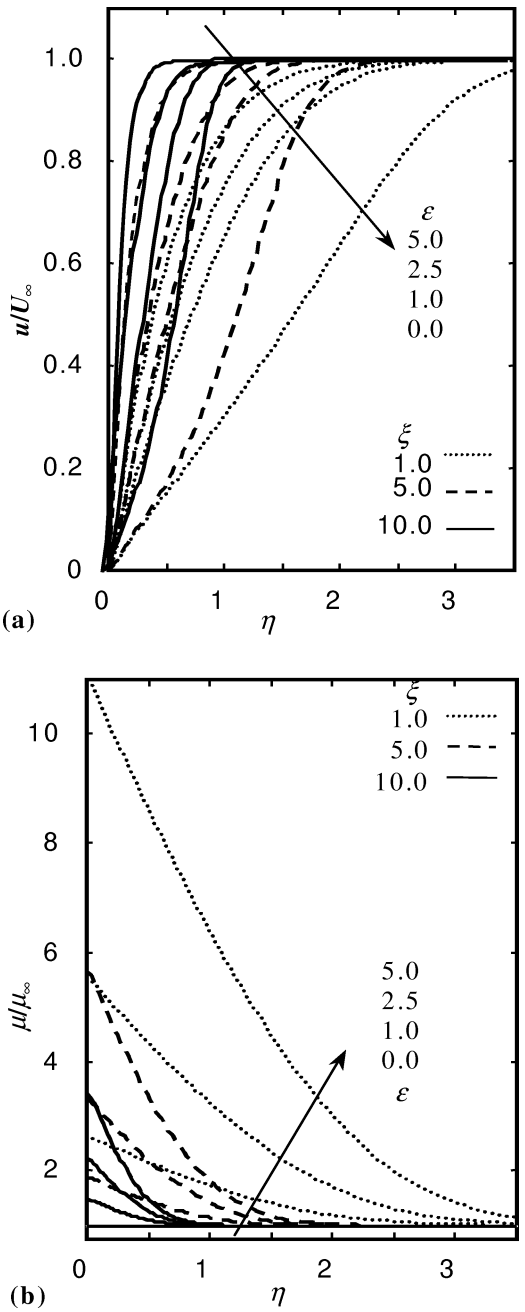

Figure 2. (a) The dimensionless velocity and (b) the dynamic viscosity distribution for different $\varepsilon = 0.0, 1.0, 2.5, 5.0$ at $Pr = 0.7$, $m = 0.5$ and $\gamma = 0.5$ while $\xi = 1.0, 5.0, 10.0$.

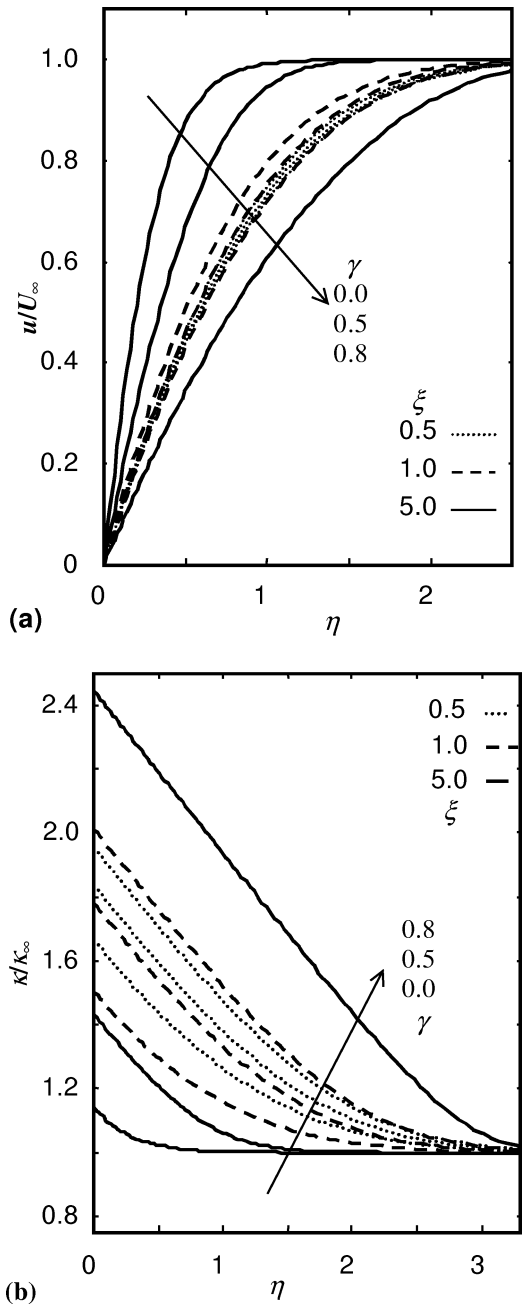

Figure 3. (a) The dimensionless velocity and (b) the thermal conductivity distribution for different $\gamma = 0.0, 0.5, 0.8$ at $Pr = 0.7$, $m = 0.5$ and $\varepsilon = 0.5$ while $\xi = 0.5, 1.0, 10.0$.

the velocity decreases by 59.84, 79.30 and 86.83 % with an increase in the viscosity parameter ε from 0.0 to 1.0, 2.5 and 5.0, respectively; the corresponding increases of viscosity are 29, 95, 75.92 and 146.96 %.

The effect of changes in the thermal conductivity variation parameter, $\gamma = 0.0, 0.5, 0.8$, on the dimensionless velocity function u/U_∞ and thermal conductivity function κ/κ_∞ against η at $\xi = 0.5, 1.0, 5.0$ for the fluid with $Pr = 0.7$, $m = 0.5$ and $\varepsilon = 0.5$ is shown in *figures 3(a)* and *3(b)*. In these figures the solid, dashed and dotted curves are used to represent the aforementioned physical variables for $\xi = 5.0$, $\xi = 1.0$ and $\xi = 0.5$, respectively. From *figure 3(a)* it can be seen that if the thermal conductivity variation parameter increases, then the velocity of the fluid decreases. For different values of γ, the profiles become closer in the intermediate region as ξ decreases, and at small values of ξ the effect of changes in γ is insignificant. On the other hand, from *figure 3(b)* it may be seen that when the thermal conductivity variation parameter γ increases, the thermal conductivity distribution also increases. These profiles all asymptote to the unit value near the edge of the boundary layer, since this is where ambient conditions are recovered. Again, for experimental interest, we show the changes in the velocity and thermal conductivity with the increase of thermal conductivity variation parameter as percentages. For example, at $Pr = 0.7$, $m = 0.5$, $\varepsilon = 0.5$, $\xi = 10.0$ and $\eta = 0.2$ the velocity decreases by 37.83 and 71.36 % with the increase in the thermal conductivity variation parameter γ from 0.0 to 0.5 and 0.8 respectively; the corresponding increases in thermal conductivity are 33.23 and 214.52 %.

4. CONCLUSIONS

The effects of temperature dependent viscosity and thermal conductivity on forced convection boundary layer flow about a wedge have been studied theoretically. The local nonsimilarity equations governing the flow in the leading edge as well as in the asymptotic regime are solved using suitable perturbation methods. Numerical solutions of the equations governing the flow in the forced convection have also been obtained by the use of an implicit finite difference method. The perturbation solutions obtained for the two extreme regimes are found to be in excellent agreement with the fully numerical solutions in their respective domains of validity. From the present investigation the following conclusions may be drawn:

1. In the entire ξ range, both the local skin-friction coefficient and the local Nusselt number increase as ξ increases for all ε, γ and m.

2. The local skin friction coefficient and the local Nusselt number decrease with the increase of ε for all ξ.

3. The local friction coefficient and the Nusselt number increase as γ decreases for all values of ξ.

4. The velocity decreases and the corresponding viscosity of the fluid increases near the surface owing to increase in the value of ε.

5. The velocity increases and the corresponding viscosity of the fluid decreases near the surface owing to an increase of ξ.

6. The velocity decreases and the corresponding thermal conductivity of the fluid increases near the surface owing to an increase in the value of ε.

7. The dimensionless dynamic viscosity as well as the thermal conductivity of the fluid approache unity at the outer edge of the boundary layer for values of all the pertinent parameters, which is trivial.

Acknowledgement

One of the authors (M.S. Munir) would like to acknowledge and express his gratitude to the Bose Centre for Advanced Studies and Research, University of Dhaka, for providing financial support during the period in which this research was undertaken.

REFERENCES

[1] Lin H.T., Lin L.K., Similarity solutions for laminar forced convection heat transfer from wedges to fluids of any Prandtl number, Int. J. Heat Mass Tran. 30 (1987) 1111–1118.

[2] Schlichting H., Boundary Layer Theory, 7th Ed., McGraw-Hill, New York, 1979, p. 156.

[3] Koh J.C.Y., Hartnett J.P., Skin-friction and heat transfer for incompressible laminar flow over porous wedges with suction and variable wall temperature, Int. J. Heat Mass Tran. 2 (1961) 185–198.

[4] Watanabe T., Thermal boundary layer over a wedge with uniform suction or injection in forced flow, Acta Mechanica 83 (1990) 119–126.

[5] Yih K.A., Uniform suction/blowing effect on the forced convection about a wedge: uniform heat flux, Acta Mechanica 128 (1998) 173–181.

[6] Gary J., Kassoy D.R., Tadjeran H., Zebib A., The effect of significant viscosity variation on convective heat transport in water-saturated porous media, J. Fluid Mech. 117 (1982) 233–249.

[7] Mehta K.N., Sood S., Transient free convection flow with temperature dependent viscosity in a fluid saturated porous medium, Int. J. Engrg. Sci. 30 (1992) 1083–1087.

[8] Hady F.M., Bakier A.Y., Gorla R.S.R., Mixed convection boundary layer flow on a continuous flat plate with variable viscosity, Heat Mass Tran. 31 (1996) 169–172.

[9] Kafoussias N.G., Williams E.W., The effect of temperature-dependent viscosity on the free convective laminar boundary layer flow past a vertical isothermal flat plate, Acta Mechanica 110 (1997) 123–137.

[10] Kafoussias N.G., Rees D.A.S., Numerical study of the combined free and forced convective laminar boundary layer flow past a vertical isothermal flat plate with temperature dependent viscosity, Acta Mechanica 127 (1998) 39–50.

[11] Severin J., Herig H., Onset of convection in the Raleigh–Benard flow with temperature dependent viscosity: an asymptotic approach, ZAMP (1999) (in press).

[12] Severin J., Herig H., Raleigh–Benard Konvektion bei variabler Viskosität; eine asymptotische Theorie, ZAMM (1999) (in press).

[13] Hossain M.A., Kabir S., Rees D.A.S., Natural convection flow from vertical wavy surface with variable viscosity, ZAMP (1999) (in press).

[14] Hossain M.A., Munir M.S., Mixed convection flow of a viscous fluid from a vertical flat plate with temperature dependent viscosity, Int. J. Therm. Sci. (2000) (in press).

[15] Hossain M.A., Munir M.S., Takhar H.S., Natural convection flow of a viscous fluid about a truncated cone with temperature dependent thermal conductivity, Acta Mechanica (1999) (in press).

[16] Hossain M.A., Munir M.S., Hafiz M.Z., Takhar H.S., Flow of a viscous incompressible fluid with temperature dependent viscosity past a permeable wedge with uniform surface heat flux, Heat Mass Tran. (2000) (in press).

[17] Kays W.M., Convective Heat and Mass Transfer, McGraw-Hill, New York, 1966, p. 362.

[18] Arunachalam M., Rajappa N.R., Thermal boundary layer in liquid metals with variable thermal conductivity, Appl. Sci. Res. 34 (1978) 179–187.

[19] Chaim T.C., Heat transfer in a fluid with variable thermal conductivity over a linearly stretching sheet, Acta Mechanica 129 (1998) 63–72.

[20] Charradeau.

[21] Keller H.B., Numerical methods in boundary layer theory, Ann. Rev. Fluid. Mech. 10 (1978) 417–433.